SAE International™

# Chassis Torsional Stiffness: Analysis of the Influence on Vehicle Dynamics

2010-01-0094
Published
04/12/2010

Enrico Sampo', Aldo Sorniotti and Andrew Crocombe
University of Surrey



## ABSTRACT

It is universally recognized that torsional stiffness is one of the most important properties of a vehicle chassis, [1]. There are several reasons for which high chassis stiffness is preferable. Lack of chassis torsional stiffness affects the lateral load transfer distribution, it allows displacements of the suspension attachment points that modify suspension kinematics and it can trigger unwanted dynamic effects like resonance phenomena or vibrations, [2].

The present paper introduces two analytical vehicle models that constitute an efficient tool for a correct evaluation of the main effects of chassis torsional stiffness on vehicle dynamics. In the first part an enhanced steady-state vehicle model is derived and employed for the analysis of the vehicle handling. The model takes account of chassis torsional stiffness for the evaluation of the lateral load transfer and, by means of the concept of the axle cornering stiffness, includes the effects of tire non-linear behavior.

In the second part of the paper a linear four-degrees-of-freedom model is presented. The frequency response of the vehicle subjected to steering inputs is analyzed. The influence of chassis torsional stiffness on the modes of motion and their dependency on the vehicle parameters is investigated.

Simulations of the behavior of two real vehicles are introduced and a sensitivity analysis is presented.

## INTRODUCTION

Very often, when a new racing or sports car is presented, the quality of its chassis is praised by giving figures of its torsional stiffness. It is in fact known that in order to obtain good handling performances, stiffness, together with lightness and weight distribution is one of the most important properties of a chassis, [3].

Depending on its shape and manufacture, a chassis exhibits a certain resistance to deformation, which is stiffness. The term chassis stiffness or rigidity generally indicates resistance to bending or flexing while torsional stiffness indicates resistance to twisting. According to Costin and Phipps, [3], however, "it is difficult to imagine a chassis that has enough torsional stiffness without having ample rigidity in bending" so that "the criterion of chassis design, and in fact the primary function of a high-performance chassis, is torsional rigidity". As a consequence, the present papers only deals with torsional stiffness and the terms *stiffness* and *torsional stiffness* are considered synonymous.

There are several factors that make the torsional rigidity of the chassis an important figure in vehicle dynamics. A chassis with low torsional stiffness generates different problems:

- the control of lateral load transfer distribution is difficult and the vehicle does not respond as expected to setup changes;
- displacements of the suspension attachment points occur, so that the desired control of the movement of the tires cannot be guaranteed;
- dynamic effects like vibrations can occur;
- fatigue phenomena are more marked;
- ride quality is poor.

Depending on the class of vehicle considered, these problems can be more or less important. The present paper is focused on sports and racing vehicles for which the control of lateral load transfer and the dynamic effects are particularly relevant. Only these issues are therefore considered.

***Table 1. Roll stiffness and chassis torsional stiffness for different groups of vehicles (indicative values).***

| Vehicle | Roll stiffness [Nm/deg] | Chassis torsional stiffness [Nm/deg] | Chassis / roll stiffness ratio |
|---|---|---|---|
| Formula SAE car, [4] | 500 - 1500 | 1000 - 5000 | 2 - 8 |
| Passenger car, [5] | 500 - 2500 | 5000 - 20000 | 4 - 10 |
| Winston Cup racing car, [6] | 1500 - 2500 | 15000 - 30000 | 6 - 12 |
| Sports car, [1] | 500 - 5000 | 15000 - 40000 | 3 - 8 |
| Formula One car, [1] | 1500 - 7500 | 10000 - 100000 | 6 - 12 |

In spite of the importance of the problem, the literature on the subject is rather scant. There exist some rules of thumb, diffused in the racing community, which suggest some figures about the minimum chassis torsional that ensures the designer that the above-mentioned problems are avoided. However, they cannot be used for optimization purposes or for advanced design.

<table 1 here>

It is known that the ratio of chassis torsional stiffness to suspension roll stiffness is a good indicator of relative chassis stiffness. Some indicative values of vehicle suspension roll stiffness and chassis torsional stiffness for different groups of vehicles are reported in Table 1. The fraction of roll due to tire deflection is here not considered. The table confirms that ratio of chassis torsional stiffness to suspension roll stiffness can be used to compare different vehicles and to develop general design rules. However, it also confirms that a rather wide range of values for each class of vehicles can be found and that, as a consequence, a more detailed analysis is necessary.

In their paper, Deakin et al. suggested an empirical formula for the estimation of the minimum ratio of chassis stiffness to roll stiffness that ensures a good control of the lateral load transfer distribution, [4]. The paper, however, does not take into account that the sensitivity of the lateral load distribution towards the chassis stiffness also depends on roll axis position. Other papers are focused on chassis design and torsional stiffness optimization, [6,7,8]; others are focused on particular problems related to the design of trucks, [9,10] but none of them presents a detailed and complete analysis of the problem.

Vehicle dynamics modeling plays nowadays a very important role in vehicle design. The employed models usually consider the chassis of the vehicle as an infinitely stiff body. This assumption is generally satisfactory when road cars are analyzed but it cannot be universally accepted when sports and racing cars are considered. The problem is often analyzed by means of advanced multi-body codes, [11,12]. This technique requires a detailed analysis of the structure of the vehicle to be carried on by means of Finite Element Methods, the extraction of the modal shapes of the chassis and their use within the chosen multi-body code. This approach leads to accurate results but it requires a large number of inputs that are not available during the preliminary phase of the design process. The present paper instead, introduces two analytical models that not only require a minimum amount of information, but they also permit a straightforward understanding of the problem.

# STEADY-STATE VEHICLE HANDLING

## LATERAL LOAD TRANSFER

Steady-state vehicle handling is greatly influenced by lateral load transfer distribution, [13,14]. Lateral load transfer occurs every time a vehicle is engaged in a cornering maneuver and consists of a partial shift of the weight of the vehicle from the tires on the inner side of the track to those on the outer side. Because of the non-linear dependency of the tire cornering stiffness on the tire load, an increase of the lateral load transfer applied to an axle decreases the axle cornering stiffness, [5]. The lateral load transfer is usually not equally distributed between the front and the rear axles; as a consequence, its distribution is a primary parameter for tuning the vehicle behavior.

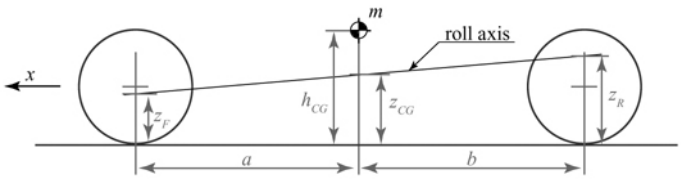


***Figure 1. Single mass model for lateral load transfer.***

## Model with infinitely stiff chassis

A model for the evaluation of vehicle lateral load transfer under the hypothesis of an infinitely rigid chassis is presented by Milliken, [1]. According to this model, represented in Figure 1, it is possible to control the lateral load transfer distribution by tuning the roll stiffness distribution and the roll axis position. The following assumptions are introduced:

- a lateral load applied along the roll axis does not produce roll;
- front and rear roll rates are measured independently;
- the roll centers and the centre of gravity are located on the centerline of the vehicle;
- unsprung masses are neglected;
- the gravity term associated with roll angle is neglected;
- front and rear track widths are considered coincident;
- all the lines normal to the roll axis are considered vertical.

Under these assumptions, the total lateral load transfer generated during cornering can be evaluated by means of the following equation:

$$\Delta F_z = \frac{m h_{CG}}{t} a_y \qquad (1)$$

where $m$ is the vehicle mass, $h_{CG}$ the height of its center of gravity and $t$ its track width. The lateral load transfer at the front and at the rear axle can be evaluated as:

$$\Delta F_{zF} = \frac{m}{t}\left(\frac{k_F}{k_F + k_R} d_{CG} + \frac{b}{l} z_F\right) a_y \qquad (2)$$

$$\Delta F_{zR} = \frac{m}{t}\left(\frac{k_R}{k_F + k_R} d_{CG} + \frac{a}{l} z_R\right) a_y \qquad (3)$$

where $k_F$ and $k_R$ are respectively the front and rear roll stiffnesses, $d_{CG} = h_{CG} - z_{CG}$ is the distance between the center of gravity and the roll axis, and $a$ and $b$ represent, respectively, the front and the rear semi wheelbases.

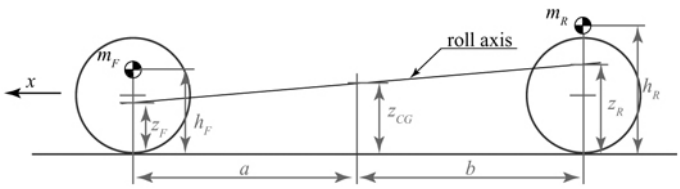


***Figure 2. Two mass model for lateral load transfer.***

## Two mass model with infinitely stiff chassis

The model described in Equations (2) and (3) is equivalent to a two mass model in which the masses $m_F$ and $m_R$ represent the front and the rear halves of the vehicle, see Figure 2. They are respectively equal to:

$$m_F = \frac{b}{l} m \qquad m_R = \frac{a}{l} m \qquad (4)$$

According to the present model, lateral load transfer generated by the one half of the vehicle is withstood by the front and rear roll stiffnesses that can be seen as connected *in parallel*. As a consequence, Equations (2) and (3) for the evaluation of the steady-state lateral load transfer can be rewritten as:

$$\Delta F_{zF} = \frac{m}{t}\left(\frac{k_F}{k_F + k_R} \frac{b}{l} d_F + \frac{k_F}{k_F + k_R} \frac{a}{l} d_R + \frac{b}{l} z_F\right) a_y \qquad (5)$$

$$\Delta F_{zR} = \frac{m}{t}\left(\frac{k_R}{k_F + k_R} \frac{b}{l} d_F + \frac{k_R}{k_F + k_R} \frac{a}{l} d_R + \frac{a}{l} z_R\right) a_y \qquad (6)$$

where $d_F$ and $d_R$ represent the distances between the mass centers of the front and of the rear parts of the chassis and the respective roll centers, the heights of which are $z_F$ and $z_R$.

## Two mass model with finite chassis stiffness

A model that includes chassis torsional stiffness can be developed by substituting the link which connects the front and the rear axles by means of a torsion spring of stiffness $k_C$. The model can be easily derived from Equations (5) and (6). It is in fact possible to notice that the fraction of the lateral load transfer generated by the front part of the vehicle and transmitted to the rear axle encounters, along its load path, the torsional spring which represents the chassis stiffness. As a consequence the spring which represents the chassis stiffness can be seen as *in series* with the rear axle roll

stiffness. A similar argument is valid for the fraction of the lateral load generated by the rear half of the vehicle. It is therefore possible to write the equation for the lateral load transfer of the front axle:

$$\Delta F_{zF} = \frac{m}{t}\left( \frac{k_F}{k_F + \frac{k_R k_C}{k_R + k_C}} \frac{b}{l} d_F + \frac{\frac{k_F k_C}{k_F + k_C}}{k_R + \frac{k_F k_C}{k_F + k_C}} \frac{a}{l} d_R + \frac{b}{l} z_F \right) a_y \tag{7}$$

Similarly, the lateral load transfer of the rear axle becomes:

$$\Delta F_{zR} = \frac{m}{t}\left( \frac{\frac{k_R k_C}{k_R + k_C}}{k_F + \frac{k_R k_C}{k_R + k_C}} \frac{b}{l} d_F + \frac{k_R}{k_R + \frac{k_F k_C}{k_F + k_C}} \frac{a}{l} d_R + \frac{a}{l} z_R \right) a_y \tag{8}$$

Naturally, Equations (7) and (8) are equivalent to Equations (5) and (6) if $k_C$ tends to infinity. Furthermore, it is possible to demonstrate that the equivalence is also verified if the following relationship is satisfied:

$$\frac{k_F}{k_R} = \frac{b}{a}\frac{d_F}{d_R} \tag{9}$$

The roll moments generated by the front and the rear parts of the chassis can be written as:

$$M_F = \frac{b}{l} m\, d_F\, a_y \qquad M_R = \frac{a}{l} m\, d_R\, a_y \tag{10}$$

and it is therefore straightforward to demonstrate that the ratio $M_F / M_R$ corresponds to the right hand side of Equation (9). It is therefore possible to conclude that the chassis torsional stiffness does not affect the lateral load transfer distribution if the ratio of front to rear torsional stiffness is equal to the ratio of front to rear roll moment. In practice however, this condition is hardly ever satisfied. This is due to several design constraints, but also to roll axis displacements and to road irregularities.

As shown, it is useful to normalize the front and the rear roll stiffness, as well as the chassis stiffness, to the total vehicle roll stiffness and the lateral load transfers to the total vehicle load transfer. The following quantities are therefore defined:

$$\kappa_F = \frac{k_F}{k_F + k_R},\ \kappa_R = \frac{k_R}{k_F + k_R},\ \kappa_C = \frac{k_C}{k_F + k_R},\ \chi_F = \frac{\Delta F_{zF}}{\Delta F_z},\ \chi_R = \frac{\Delta F_{zR}}{\Delta F_z} \tag{11}$$

## Axle cornering stiffness

Tire behavior can be described, under the assumption of small side slip and null camber angles, by means of the linear expression, [1,5]:

$$F_{yT} = C_{\alpha T}\, \alpha \tag{12}$$

in which $F_{yT}$ represents tire cornering force, $C_{\alpha T}$ tire cornering stiffness and $\alpha$ slip angle.

Cornering stiffness is not constant but it depends on tire normal load. This dependency, named load sensitivity, is usually a non-linear function commonly approximated by means of a linear, a polynomial or an exponential model, [5]. A second order polynomial fit is here adopted:

$$C_{\alpha T} = \xi_{\alpha 0} + \xi_{\alpha 1} F_{zT} + \xi_{\alpha 2} F_{zT}^2 \tag{13}$$

It is therefore possible to write the axle cornering stiffness $C_\alpha$ as a function of the axle load transfer:

$$C_\alpha = C_{\alpha 0} + 2\xi_{\alpha 2} \Delta F_z^2 \tag{14}$$

where $C_{\alpha 0}$ represents the axle cornering stiffness when no load transfer occurs. As the coefficient $\xi_{\alpha 2}$ is always negative, the presence of a load transfer always decreases the axle cornering stiffness. It is therefore possible to define an axle cornering stiffness decay coefficient $\eta_\alpha = -2\xi_{\alpha 2}\chi^2$ so that Equation (14) can be rewritten as:

$$C_{\alpha F} = C_{\alpha F0} + 2\xi_{\alpha F2}\chi_F^2 \Delta F_z^2 = C_{\alpha F0} - \eta_{\alpha F} \Delta F_z^2 \tag{15}$$

$$C_{\alpha R} = C_{\alpha R0} + 2\xi_{\alpha R2}\chi_R^2 \Delta F_z^2 = C_{\alpha R0} - \eta_{\alpha R} \Delta F_z^2 \tag{16}$$

## VEHICLE HANDLING

The effects of chassis torsional stiffness on the steady-state behavior of the vehicle can be analyzed by means of the same parameters typical of bicycle models. A detailed derivation of the bicycle model can be found in [1]. Only the necessary assumptions are here reported:

- no longitudinal forces are considered;
- no rolling or pitch motions are considered;
- aerodynamic effects are neglected;

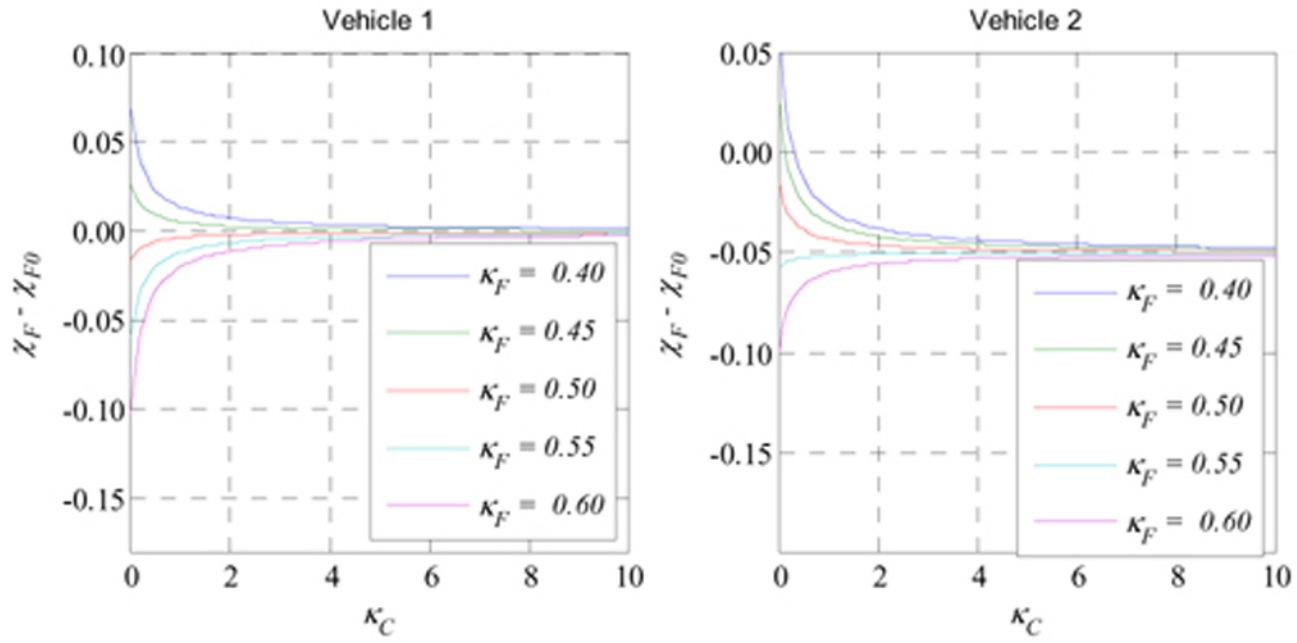


***Figure 3. Normalized difference between the front lateral load transfer obtained with different levels of chassis stiffness ($\chi_F$) and those obtained with an infinitely stiff chassis model ($\chi_{F0}$) versus chassis torsional stiffness for different values of roll stiffness distribution.***

• side slip and steering angles are considered small.

Under these hypotheses, the steady-state behavior of the vehicle can be analyzed by means of the trajectory curvature gain, defined as:

$$\frac{1}{R\delta} = \frac{1}{l}\frac{1}{1+Kv^2} \tag{17}$$

In which $K$ is the stability factor, defined as:

$$K = \frac{m}{l^2}\left(\frac{b}{C_{\alpha F}} - \frac{a}{C_{\alpha R}}\right) \tag{18}$$

By introducing Equations (15) and (16) into Equation (18) and, in turn, this into Equation (17), it is possible to obtain the vehicle curvature gain as a function of the vehicle longitudinal speed.

# RESULTS

Results are reported for two vehicles. Vehicle 1 is a light front-engine two-seater sports car with a tubular space frame; Vehicle 2 is a race vehicle developed by the University of Surrey for the 2009 edition of the English Formula Student event. The data of the two vehicles are reported in Table A1 of Appendix A.

## Influence of chassis torsional stiffness on lateral load transfer distribution

The parameter most directly affected by chassis torsional stiffness is lateral load transfer distribution. Figure 3 shows the difference between the fraction of the lateral load transfer withstood by the front axle when chassis torsional stiffness is considered and the same quantity when it is neglected. Data are plotted versus the normalized chassis torsional stiffness for different values of roll stiffness distribution.

The analysis of the graphs shows that, unless the torsional stiffness of the chassis is extremely low ($\kappa_C < 1$) the error made if the chassis torsional stiffness is neglected is within 5% of the total load transfer. This is valid for both vehicles. Furthermore, if the chassis is very stiff ($\kappa_F > 5$) the error made is extremely small. If light sports or race cars are however considered, values of $\kappa_C$ included in the range 1-5 are rather common, see Table 1. It is therefore important to take account of the chassis stiffness if a good estimation of the lateral load transfer distribution is desired.

<figure 3 here>

<figure 4 here>

Influence of roll stiffness distribution on lateral load transfer distributionFigure 4 reports the difference between the lateral load transfer distribution when chassis stiffness is considered

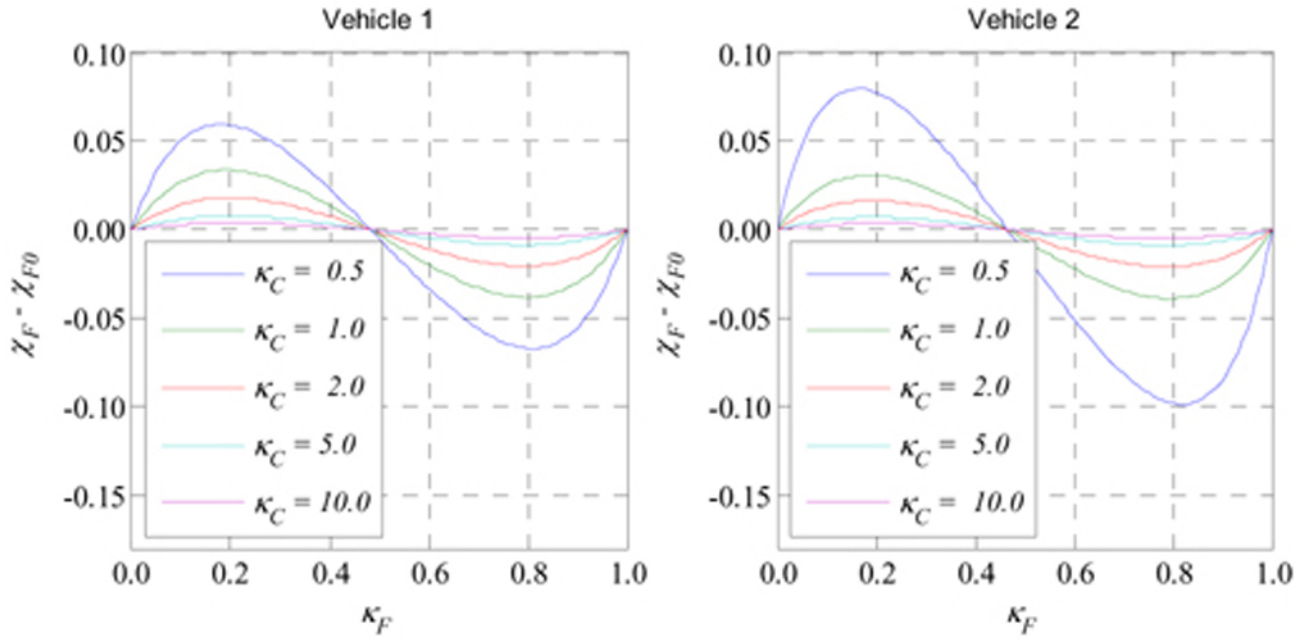


***Figure 4. Normalized difference between the front lateral load transfer obtained with different levels of chassis stiffness ($\chi_F$) and those obtained with an infinitely stiff chassis ($\chi_{F0}$) versus roll stiffness distribution for different values of chassis torsional stiffness.***

($\chi_F$) and when it is neglected ($\chi_{F0}$) versus roll stiffness distribution. Different values of chassis torsional stiffness are considered. The graphs relative to Vehicle 1 and Vehicle 2 show very similar trends; first the absolute value of $\chi_F - \chi_{F0}$ grows as $\kappa_F$ moves away from the values expressed in Equation (9), (respectively $\kappa_{F0} = 0.48$ for Vehicle 1 and $\kappa_{F0} = 0.49$ for Vehicle 2) and then it decreases when $\kappa_F$ tends to 0 or to 1. In both these situations, in fact, the torque transmitted through the chassis is null.

If the analysis is limited to a reasonable range of values of $\kappa_F = 0.25 - 0.75$, it is possible to say that a lack of chassis torsional stiffness causes a reduction of the effect of roll stiffness tuning on lateral load transfer distribution which is directly proportional to the difference between $\kappa_F$ and $\kappa_{F0}$.

It is normal practice to tune the steady-state behavior of the vehicle by modifying the roll stiffness distribution. Tuning is greatly eased if the sensitivity of the lateral load transfer distribution versus the roll stiffness distribution is constant. This is possible only if the chassis is infinitely stiff; a quasi-linear sensitivity is however accepted. The above-mentioned sensitivity can be evaluated as the tangent to the curves of Figure 4: it is higher for values of $\kappa_F$ close to $\kappa_{F0}$ and it is largely affected by the chassis compliance up to $\kappa_C = 5$.

<figure 5 here>

## Influence of roll axis position on lateral load distribution

According to Equations (7) and (8), lateral load transfer is partially controlled by roll axis position. Figure 5 reports the value of $\kappa_F - \kappa_{F0}$ versus chassis torsional stiffness for different values of roll axis height. The roll axis is here considered parallel to the ground ($z_F = z_R$).

For both vehicles, lower or negative values of roll center height emphasize the effect of chassis compliance. This effect however is more important for Vehicle 2. According to Equation (9), there exists a roll axis position for which the effect of chassis stiffness is null. It is possible to show that its value is given by the expression:

$$z_F = z_R = \frac{bk_R h_F - ak_F h_R}{bk_R - ak_F} \qquad (19)$$

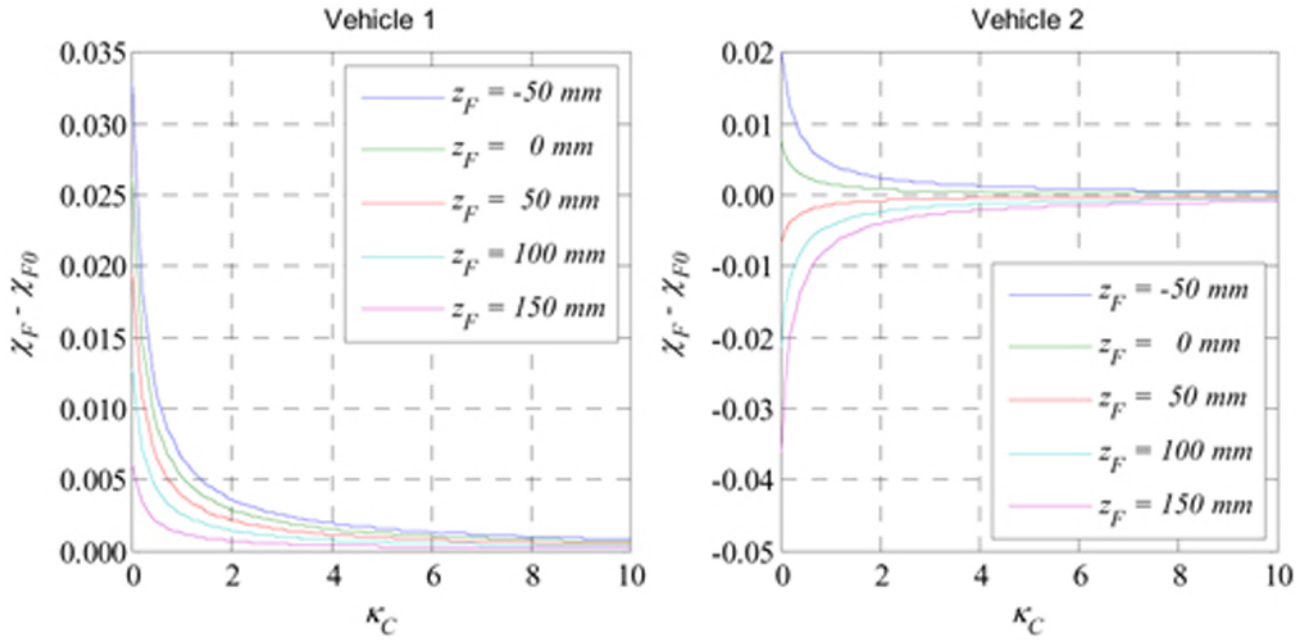


***Figure 5. Normalized difference between the front lateral load transfer obtained with different levels of chassis stiffness ($\chi_F$) and those obtained with an infinitely stiff chassis ($\chi_{F0}$) versus roll stiffness distribution for different values of roll axis height.***

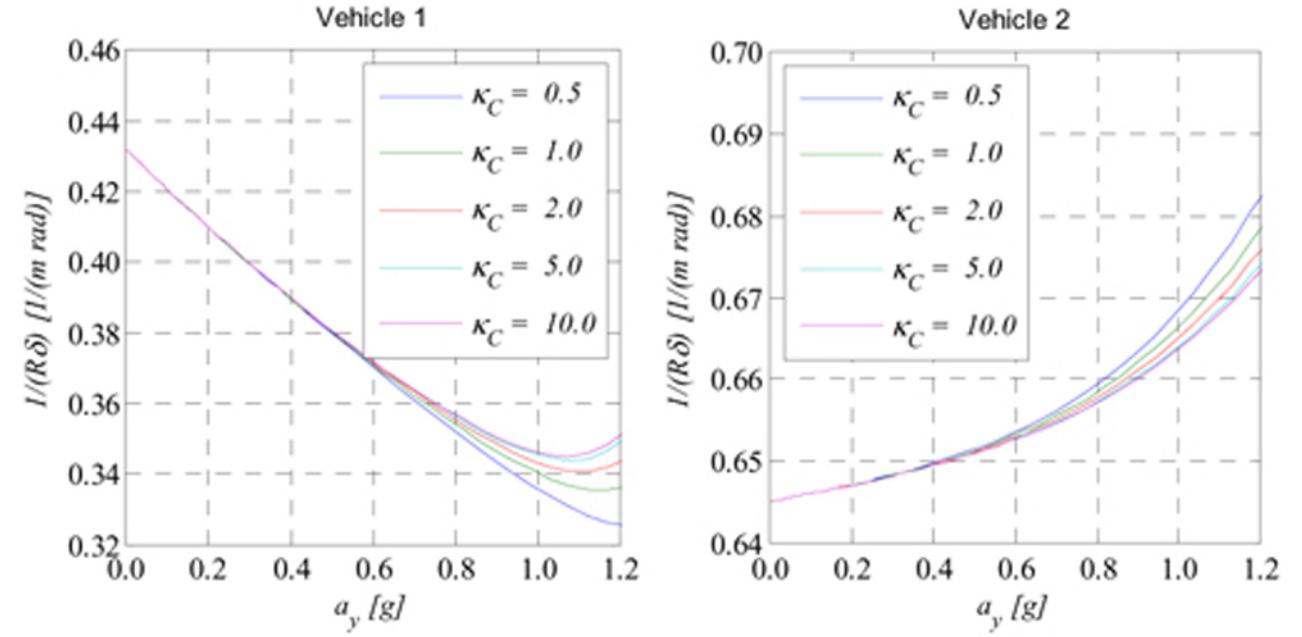


***Figure 6. Trajectory curvature gain versus lateral acceleration for different values of chassis torsional stiffness.***

Equation (19) leads to values of $z_F = z_R = 195$ mm for Vehicle 1 and $z_F = z_R = 27$ mm for Vehicle 2.

<figure 6 here>

## Influence of chassis stiffness on vehicle handling

The developed model permits the analysis of the influence of the chassis stiffness on the steady-state vehicle characteristics, see Equation (17). The trajectory curvature gain versus lateral acceleration of Vehicle 1 and Vehicle 2 are plotted in Figure 6. As expected, Vehicle 1 has a natural tendency to understeer while Vehicle 2 tends to oversteer. For both vehicles, the over- or under-steer behavior is reduced

through the tuning of the roll stiffness distribution. The presence of the chassis compliance reduces the balancing effect of roll stiffness distribution and for low values of chassis torsional stiffness, Vehicle 1 has a more marked tendency to understeer, while Vehicle 2 has a more marked tendency to oversteer. For both vehicles, it seems that no sensible effects can be noticed for values of $\kappa_C > 5$.

# LINEAR ANALYSIS

A linear model for the analysis of the frequency response and of the stability of the vehicle is presented in the present paragraph.

## Linear model

A vehicle model with roll and chassis torsional stiffness, described in Figure 7, is employed. The model has four degrees of freedom: lateral motion ($y$), yaw ($\psi$), roll of the front ($\phi_F$) and roll of the rear ($\phi_R$) part of the sprung mass. A similar model was described by Hasegawa et al., [9] and employed for the study of the stability of heavy good vehicles.

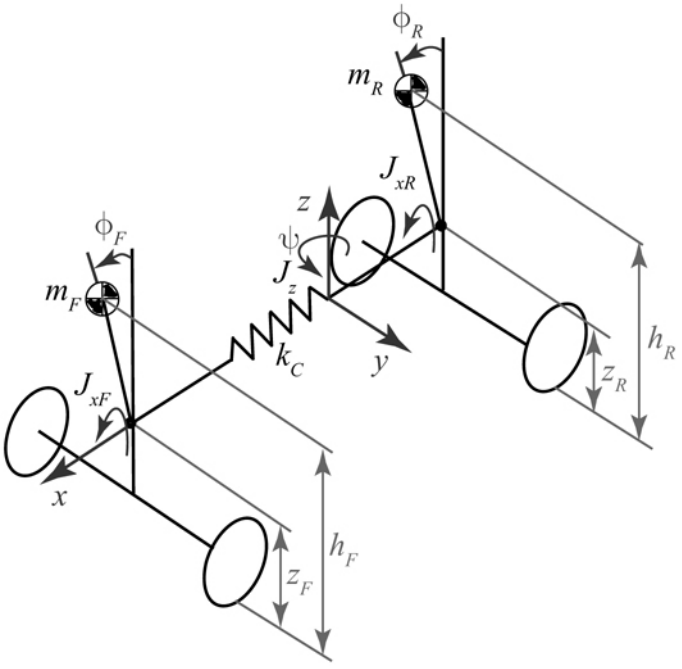


***Figure 7. Linear model.***

Referring to Figure 7, it is possible to demonstrate that the equations of motion can be written as:

$$\begin{cases} m\left(\ddot{y}+v\dot{\psi}\right)-m_F d_F\ddot{\phi}_F-m_R d_R\ddot{\phi}_R=F_{yF}+F_{yR} \\ J_z\ddot{\psi}-m_F a d_F\ddot{\phi}_F+m_R b d_R\ddot{\phi}_R=F_{yF}a-F_{yR}b \\ J_{xF}\ddot{\phi}_F-m_F d_F\left(\ddot{y}+v\dot{\psi}-a\ddot{\psi}\right)+k_F\phi_F+c_F\dot{\phi}_F+k_C\left(\phi_F-\phi_R\right)=0 \\ J_{xR}\ddot{\phi}_R-m_R d_R\left(\ddot{y}+v\dot{\psi}+b\ddot{\psi}\right)+k_R\phi_R+c_R\dot{\phi}_R-k_C\left(\phi_F-\phi_R\right)=0 \end{cases} \quad (20)$$

where $m_F$ and $m_R$ represent, respectively, the front and the rear parts of the vehicle, $F_{yF}$ and $F_{yR}$ the front and rear cornering forces, $J_{xF}$ and $J_{xR}$ respectively the front and rear roll moments of inertia while $c_F$ and $c_R$ are the front and rear roll damping. As the internal damping of materials used in chassis manufacturing is usually negligible, no chassis damping is included. Tire cornering forces are evaluated by means of the linear approximation introduced in Equation (12) with a constant cornering stiffness and under the hypothesis of null camber angles. The side slip angles are calculated using the equations:

$$\alpha_F=\delta-\frac{\dot{y}+a\dot{\psi}}{v} \qquad \alpha_R=-\frac{\dot{y}-b\dot{\psi}}{v} \quad (21)$$

in which the $\delta$ is the front axle steering angle.

As the system is linear, Equations (20) can easily be written into a state space formulation and employed in order to study the frequency response and the root locus of the vehicle.

## Chassis natural frequency

If the torsional motion of chassis is considered decoupled from the main chassis motion, it is possible to evaluate the chassis natural frequency by means of a two degree of freedom model. If the influence of the roll stiffness is neglected, the equations of motion read, [6]:

$$\begin{cases} J_{xF}\ddot{\phi}_F+k_C\left(\phi_F-\phi_R\right)=0 \\ J_{xR}\ddot{\phi}_R-k_C\left(\phi_F-\phi_R\right)=0 \end{cases} \quad (22)$$

The natural frequency of the chassis can therefore be found by solving the characteristic equation associated with the system of Equation (22). The evaluated frequency corresponds to the torsion mode of the chassis when it is not installed on the vehicle because it does not include the presence of the front and rear roll stiffnesses.

A more accurate model can be derived if the front and the rear roll stiffnesses and the roll damping are included:

$$\begin{cases} J_{xF}\ddot{\phi}_F + k_F\phi_F + c_F\dot{\phi}_F + k_C\left(\phi_F - \phi_R\right) = 0 \\ J_{xR}\ddot{\phi}_R + k_R\phi_R + c_R\dot{\phi}_R - k_C\left(\phi_F - \phi_R\right) = 0 \end{cases} \quad (23)$$

The solution of the characteristic equation associated with the system of Equation (23) leads to two distinct frequencies; the lower one corresponds to the in-phase roll frequency, the higher one to the torsion mode of the chassis when it is installed on the vehicle. Interestingly, the model of Equation (23) also permits the evaluation of the damping of the chassis torsion mode. For Vehicle 1 it is $\omega_n = 8.83$ Hz and $\xi = 0.11$ while for Vehicle 2 it is $\omega_n = 18.9$ Hz and $\xi = 0.19$.

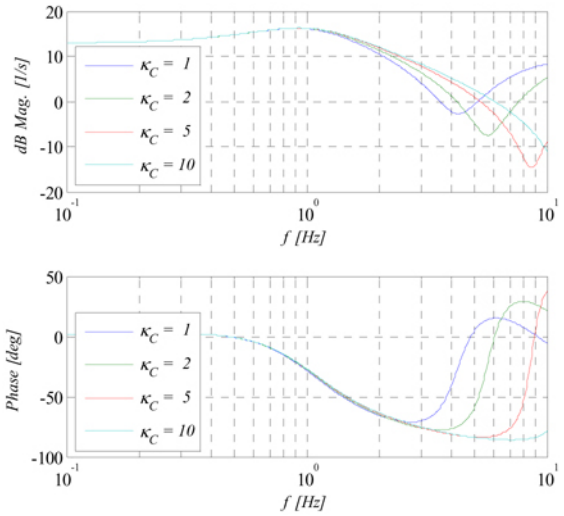


***Figure 8. Bode diagram of yaw rate response for different values of chassis torsional stiffness at 15 m/s for Vehicle 1.***

# RESULTS

The present paragraph reports the results of the linear analysis of the two vehicles described in Table A1 of Appendix A.

## Yaw rate response

First, the yaw rate response of the vehicles is analyzed. Input to the model is considered the steering angle $\delta$. Figure 8 and Figure 9 report the yaw rate response of Vehicles 1 and 2 for different values of chassis torsional stiffness at a constant speed of 15 m/s. Frequencies up to 10 Hz are plotted; the range of interest being up to 5 Hz, [15].

Both Figures show that different values of torsional stiffness affect the response of the vehicle, especially in terms of gain amplitude in the area of the resonance frequency for Vehicle 1. As Vehicle 2 is oversteering, its yaw-sideslip mode is overdamped and no resonance frequency exists. As a consequence, also the influence of $\kappa_C$ is limited. Comparing Figure 8 and Figure 9 it is also possible to notice that for lower values of chassis stiffness the phase diagram of Vehicle 1 is much more affected than the one of Vehicle 2.

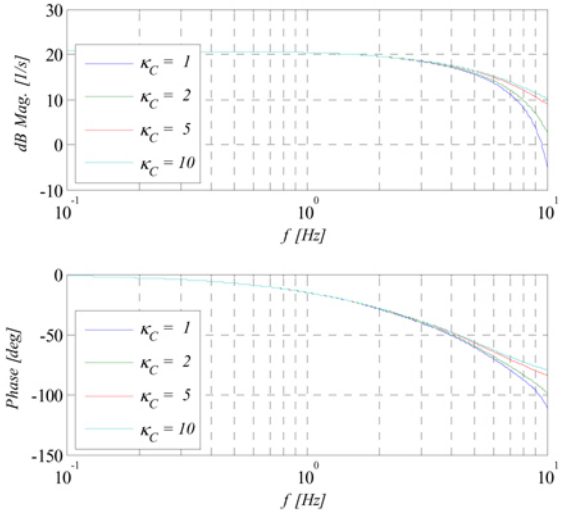


***Figure 9. Bode diagram of yaw rate response for different values of chassis torsional stiffness at 15 m/s for Vehicle 2.***

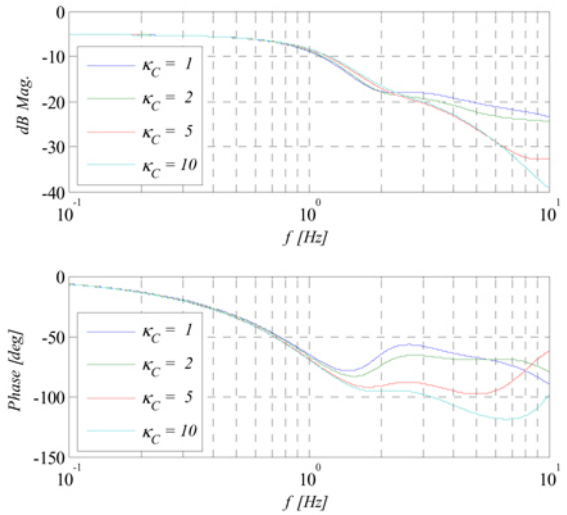


***Figure 10. Bode diagram of front roll response versus steering input for different values of chassis torsional stiffness at 15 m/s for Vehicle 1.***

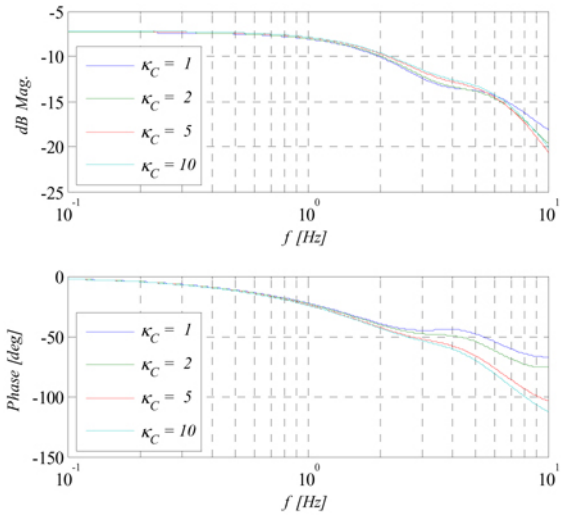


***Figure 11. Bode diagram of front roll response versus steering input for different values of chassis torsional stiffness at 15 m/s for Vehicle 2.***

## Roll response

Figure 10 shows the Bode diagram of the roll response of the front part of the chassis of Vehicle 1 at 15 m/s. As it is possible to see, the chassis compliance causes a substantial modification of the frequency response. In fact, even for values of $\kappa_C > 5$ the chassis torsional deformation increases the amplitude of the response in the high-frequency range and reduces the phase delay. A similar but less marked trend can be noticed in Figure 11 in which the frequency response of Vehicle 2 is represented.

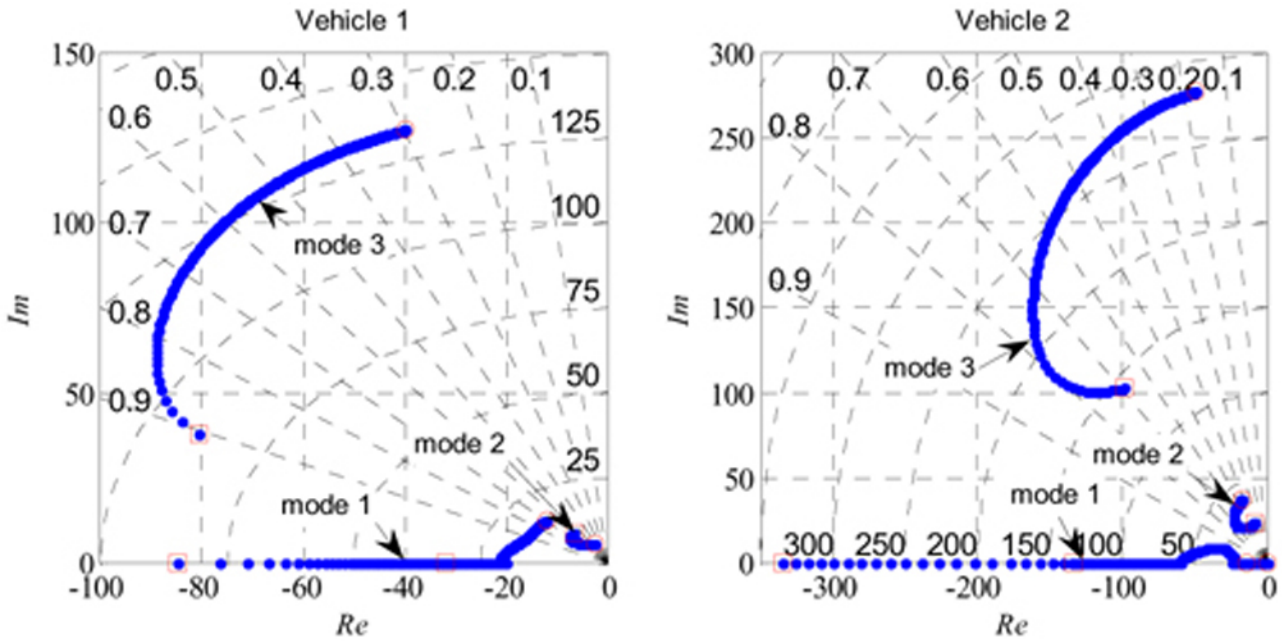


***Figure 12. Root locus of the system for $v$ from 5 m/s (□) to 50 m/s (○).***

<figure 12 here>

## Root locus analysis

When a three-degrees-of-freedom vehicle model that includes side slip, yaw and roll is considered, the motion of the vehicle can be described by using two modes, the first one being mainly side slipping and the second mainly a roll motion, [16]. When the chassis flexibility is introduced, a third mode, mainly corresponding to an out-of-phase roll motion of the two halves of the chassis can be observed. All the modes are coupled, it is however possible to distinguish them in a rather precise manner if the modal shapes are observed.

It is interesting to plot the root locus of the system for increasing values of vehicle longitudinal speed, see Figure 12. The real and the imaginary part of the eigenvalues, as well as straight lines representing constant values of damping and concentric arches corresponding to constant values of undamped natural frequencies are plotted. At low speed, the yaw-side slipping mode of both vehicles is overdamped; at higher speed it naturally becomes underdamped for the understeering vehicle (Vehicle 1). Interestingly, the presence of the chassis compliance makes mode 1 of Vehicle 2 underdamped for a limited range of speeds.

Furthermore, it seems that the chassis compliance does not affect the variation of mode 2 with speed. A sensible variation of both the natural frequency and the damping of the out-of-phase roll mode (mode 3) with speed can be observed. At low speed, the natural frequency of the mode is close to the one evaluated by means of Equation (23) but it sensibly grows with speed. A small increment of the damping can be observed at low speed for Vehicle 1; it is however possible to say that the damping is generally reduced with increasing speed.

<figure 13 here>

## Influence of chassis torsional stiffness on root locus

Figure 13 represents the root locus of Vehicles 1 and 2 at a constant speed of 15 m/s for increasing values of chassis torsional stiffness. The graphs reveal that for the understeering vehicle (Vehicle 1) the damping of the yaw and side slip mode decreases with increasing chassis stiffness; the opposite behavior is observed for the oversteering vehicle (Vehicle 2). As expected, the in-phase roll mode (mode 2) is only marginally affected by the value of the chassis stiffness. Clearly, an increment of chassis stiffness brings to higher values of the natural frequency corresponding to mode 3 while the damping of the same mode is significantly decreased when the chassis torsional stiffness is increased.

# CONCLUSIONS

In the present papers two models for the analysis of the effects of the chassis torsional stiffness on vehicle dynamics have been presented. Some effects, for example the mass and torsional stiffness distribution are taken into account in a very simplified manner; however the introduced models require a minimum amount of information and permit a first analysis of the problem.

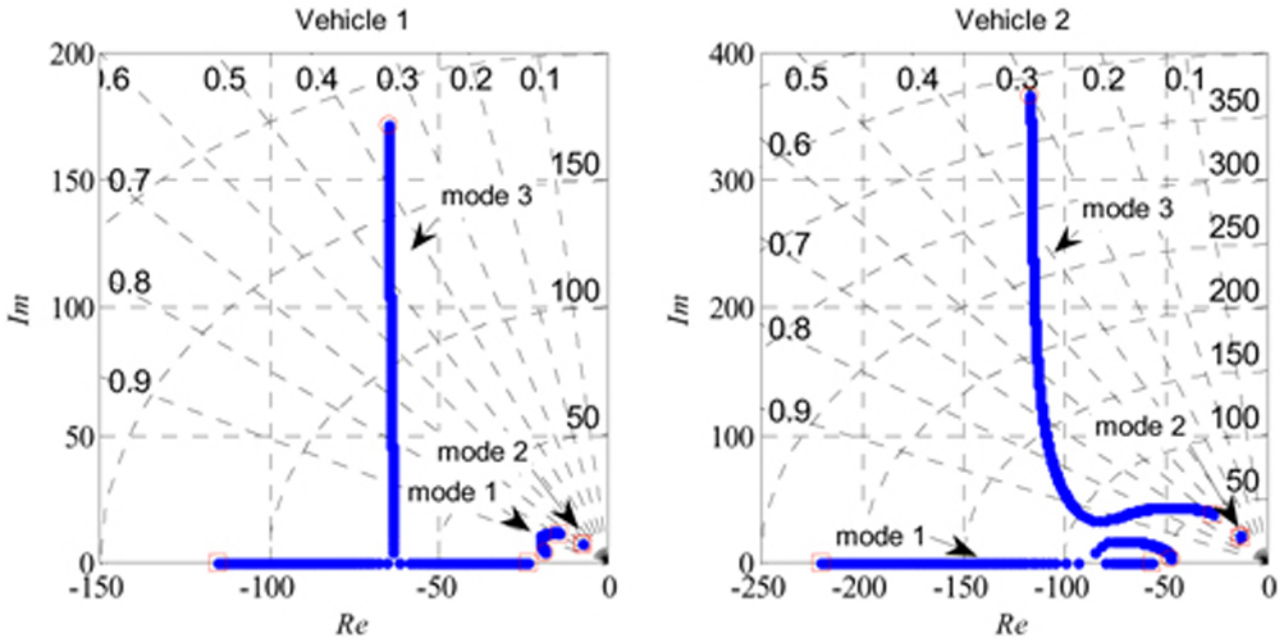


***Figure 13. Root locus of the system at constant speed of 15 m/s for $K_C$ from 1 (□) to 10 (○).***

Simulations of the behavior of two real vehicles confirm that both the steady-state characteristics and the frequency response obtained under the assumption of an infinitely stiff chassis are often inaccurate.

The effects of the chassis compliance on lateral load transfer have been analyzed; the following conclusions can be drawn:

- it is important, when sports and race vehicles are considered, to take account of the chassis torsional stiffness;
- it is possible to neglect the chassis torsional stiffness only if the ratio of chassis torsional stiffness to total roll stiffness is high (higher than 5);
- the effect of chassis torsional stiffness on lateral load transfer distribution depends on roll stiffness distribution and roll axis position;
- a lack of chassis stiffness generally makes the understeering vehicle more prone to understeer and the oversteering vehicle more prone to oversteer.

Also, the linear analysis has revealed that, within the range of frequencies achievable by a professional driver, the effects of the chassis compliance on the frequency response to driver inputs cannot be neglected. In particular:

- low chassis torsional stiffness tends to reduces the vehicle bandwidth;
- dynamic effects are important also for high values of torsional stiffness (ratio of chassis stiffness to total roll stiffness higher than 5);
- the frequency associated with the torsional mode of the chassis increases with speed; the damping of the same mode decreases with speed, leading to possible stability problems;
- the frequency of the torsional mode increases with chassis torsional stiffness; the damping of the same mode decreases with chassis torsional stiffness;
- the yaw and side slipping mode of the vehicle is sensibly affected by the chassis torsional stiffness and different trends can be observed for understeering and the oversteering vehicles;
- the pure roll mode is only marginally affected by chassis torsional stiffness.

# REFERENCES

**1.** Milliken, D.L., Kasprzak, E.M., Metz, L.D., and Milliken, W.F., "Race Car Vehicle Dynamics," SAE International, Warrendale, PA, ISBN 978-0-7680-1127-2, 1995.

**2.** Genta, G. and Morello, L., The Automotive Chassis vol. 2: System Design, Springer, New York, ISBN 978-1-4020-8673-1,2009.

**3.** Costin, M. and Phipps, D., Racing and Sports Car Chassis Design, Batsford, 1974, ISBN 978-0713404586.

**4.** Deakin, A., Crolla, D., Ramirez, J.P., and Hanley, R., "The Effect of Chassis Stiffness on Race Car Handling Balance," SAE Technical Paper 2000-01-3554, 2000.

**5.** Dixon, J., "Tires, Suspension and Handling, Second Edition," SAE International, Warrendale, PA, ISBN 978-1-56091-831-8, 1996.

**6.** Thompson, L.L., Raju, S., and Law, E.H., "Design of a Winston Cup Chassis for Torsional Stiffness," SAE Technical Paper 983053, 1998.

**7.** Riley, W.B. and George, A.R., "Design, Analysis and Testing of a Formula SAE Car Chassis," SAE Technical Paper 2002-01-3300, 2002.

**8.** Thompson, L.L., Soni, P.H., Raju, S., and Law, E.H., "The Effects of Chassis Flexibility on Roll Stiffness of a Winston Cup Race Car," SAE Technical Paper 983051, 1998.

**9.** Hasegawa, S., Kusahara, Y., and Watanabe, Y., "Influence of Vehicle Body Torsional Stiffness on Vehicle Roll Characteristics of Medium-Duty Trucks," SAE Technical Paper 902267, 1990.

**10.** Miki, S., "Method for Evaluating Stability and Handling of a Truck Considering Body Torsional Rigidity," SAE Technical Paper 881870, 1988.

**11.** Tong, Y.Y., "Vehicle Dynamic Simulations Based on Flexible and Rigid Multibody Models," SAE Technical Paper 2000-01-0114, 2000.

**12.** Ambrósio, J.A.C., and Gonçalves, J.P.C., "Complex Flexible Systems with Application to Vehicle Dynamics", *Multibody System Dynamics* 6(2): 163-182, 2001.

**13.** Clover, C.L. and Bernard, J.E., "The Influence of Lateral Load Transfer Distribution on Directional Response," SAE Technical Paper 930763, 1993.

**14.** Chu, T.W., Jones, R.P., "Analysis of Nonlinear Handling Characteristics of Automotive Vehicles with Focus on Lateral Load Transfer", *Vehicle System Dynamics* 46(Supp. 1): 17-31.

**15.** Blundell, M. and Harty, D., The Multibody Systems Approach to Vehicle Dynamics, Butterworth-Heinemann, 2004, ISBN 0750651121.

**16.** Segel, L., "Theoretical Prediction and Experimental Substantiation of the Response of the Automobile to Steering Control", *Proceedings of IMechE*, Automotive Division 1956: 310-330, 1956.

# APPENDIX A

# VEHICLE DATA

***Table A1. Vehicle data.***

| *Data* | *Description* | *Vehicle 1* | *Vehicle 2* | *Units* |
|---|---|---|---|---|
| $m$ | Vehicle mass | 700 | 270 | kg |
| $a$ | Front semi wheelbase | 1134 | 680 | mm |
| $b$ | Rear semi wheelbase | 1181 | 870 | mm |
| $J_z$ | Yaw inertia | 550 | 110 | kg m$^2$ |
| $h_{CG}$ | Centre of gravity height | 450 | 380 | mm |
| $h_F$ | Front half centre of gravity height | 420 | 310 | mm |
| $h_R$ | Rear half centre of gravity height | 481 | 470 | mm |
| $z_{CG}$ | Roll axis height in C.G. plane | 60 | 60 | mm |
| $z_F$ | Front roll centre height | 52 | 45 | mm |
| $z_R$ | Rear roll centre height | 68 | 79 | mm |
| $t_F$ | Front track width | 1500 | 1200 | mm |
| $t_R$ | Rear track width | 1502 | 1150 | mm |
| $J_{xF}$ | Front half roll inertia | 102 | 21 | kg m$^2$ |
| $J_{xR}$ | Rear half roll inertia | 124 | 33 | kg m$^2$ |
| $k_F$ | Front roll stiffness | 14400 | 17400 | Nm/rad |
| $k_R$ | Rear roll stiffness | 17600 | 15300 | Nm/rad |
| $k_C$ | Chassis torsional stiffness | 175000 | 148000 | Nm/rad |
| $c_F$ | Front roll damping | 1125 | 305 | Nms/deg |
| $c_R$ | Rear roll damping | 1375 | 225 | Nms/deg |
| $\xi_{0F}$ | Zero-order coeff. for front cornering stiffness | 0 | 0 | N/rad |
| $\xi_{1F}$ | First-order coeff. for front cornering stiffness | 31.5 | 41 | 1/ rad |
| $\xi_{2F}$ | Second-order coeff. for front cornering stiffness | -0.014 | -0.016 | 1/(N rad) |
| $\xi_{0R}$ | Zero-order coeff. for rear cornering stiffness | 0 | 0 | N/rad |
| $\xi_{1R}$ | First-order coeff. for rear cornering stiffness | 34 | 38 | 1/rad |
| $\xi_{2R}$ | Second-order coeff. for rear cornering stiffness | -0.014 | -0.016 | 1/(N rad) |

The Engineering Meetings Board has approved this paper for publication. It has successfully completed SAE's peer review process under the supervision of the session organizer. This process requires a minimum of three (3) reviews by industry experts.



ISSN 0148-7191

doi:10.4271/2010-01-0094



**SAE Customer Service:**
Tel: 877-606-7323 (inside USA and Canada)
Tel: 724-776-4970 (outside USA)
Fax: 724-776-0790
Email: CustomerService@sae.org
**SAE Web Address:** http://www.sae.org
**Printed in USA**